



# The X-ray Properties of Cataclysmic Variables

Ş. Balman<sup>1</sup>

Middle East Technical University, Department of Physics, Inonu Bulvarı, Ankara, 06531,  
Turkey e-mail: solen@astroa.physics.metu.edu.tr

**Abstract.** Cataclysmic Variables (CVs) are a distinct class of X-ray binaries transferring mass from a donor star to a compact star accretor, a white dwarf. They constitute a laboratory for accretion physics, mechanisms and disk theory together with dynamics of outflows and interaction with surrounding medium. Our understanding of the X-ray emission from CVs has shown substantial improvement in the last decade with the instruments onboard present X-ray telescopes. We have a better understanding of the boundary layers and the accretion shocks using high sensitivity instruments and/or grating X-ray spectroscopy attaining high spectral resolution yielding temperature and velocity diagnostics. In addition, high time resolution utilizes accretion mode diagnostics with characterization of the variability of the gas flow in discs. Here, I briefly review the X-ray properties of CVs with a highlight on Intermediate Polars, Dwarf Novae and Classical/Recurrent Novae.

**Key words.** Stars: novae, abundances, atmospheres, winds, outflows – Cataclysmic Variables – Intermediate Polars, Polars – White Dwarfs – Accretion, Accretion Discs – Stars: Binaries – X-rays: Stars – radiation mechanisms:thermal – stars: dwarf novae

## 1. Introduction

A Cataclysmic Variable (CV) is a close interacting binary system in which a white dwarf (WD) accretes material from its late-type low mass main sequence companion. CVs can be studied in two main classes. The accretion occurs through an accretion disc in cases where magnetic field of the WD is weak or nonexistent ( $B < 0.01$  MG), such systems are referred as nonmagnetic CVs characterized by their eruptive behavior (see Warner 1995, Warner 2003 for a review). The other class is the magnetic CVs (MCVs) divided into two subclasses according to the degree of synchronization of the binary. Polars have  $230 \text{ MG} > B > 20 \text{ MG}$  where this strong field causes the accre-

tion flow to directly channel onto the magnetic pole/s of the WD inhibiting the creation of an accretion disk (see Cropper 1990; Warner 2003) causing the WD rotation to synchronize with the binary orbit. The second class of MCVs are the Intermediate Polars which have less field strength of 1-20 MG compared with Polars and are thus asynchronous systems (Patterson 1994; Warner 2003). The space density of CVs is  $(0.5-10) \times 10^{-6} \text{ pc}^{-3}$  calculated using the X-ray luminosity function (a truncated power law) depending on the limiting X-ray flux (see Pretorius & Knigge 2011). The cumulative luminosity density of CVs in the 2-10 keV band is  $(0.8-1.4) \times 10^{27} \text{ erg s}^{-1} \text{ M}_{\odot}^{-1}$  (Sazonov et al. 2006, this value is similar in 17-60 keV range).

*Send offprint requests to:* Ş. Balman

## 2. Magnetic Cataclysmic Variables

Magnetic CVs constitute about 25% of the CV population. About 63% are Polars (P) and 37% are Intermediate Polars (IP). IPs have truncated accretion disks and as the accreting material is channeled to the magnetic poles accretion curtains form. Polars channel matter through accretion funnels to the magnetic poles. The X-ray emission is from a strong standing shock near the surface of the WD (Lamb & Masters 1979, King & Lasota 1979). The post-shock region is heated to 10-95 keV with  $L_x \leq$  a few  $\times 10^{33}$  erg s<sup>-1</sup> (Patterson 1994, Hellier 1996, Kuulkers et al. 2006, de Martino et al. 2008b, Brunschweiler et al. 2009, Yuasa et al. 2010). A subclass of IPs show soft X-ray component with blackbody emission  $kT = 30$ -100 eV (Evans & Hellier 2007, Anzolin et al. 2008, de Martino et al. 2008a, Staude et al. 2008) originating from heated WD surface. IPs are the hardest X-ray emitters reaching out to 200 keV (INTEGRAL/Swift/Suzaku- Barlow et al. 2006, Landi et al. 2009, Brunschweiler et al. 2009). As long as the dominating mechanism is a Bremsstrahlung,  $T_{max}$  of the shock yields a good approximation for the WD mass in MCVs. In general, a multi-temperature optically thin plasma of narrow and broad emission lines with low and/or high velocities in excess of 1000 km s<sup>-1</sup> at electron densities  $> 10^{12}$  cm<sup>-3</sup> are typically detected (an isobaric cooling flow type plasma emission or photoionized gas dominated plasma has been observed, e.g., Mukai et al. 2003, Luna et al. 2010). A Compton reflection component at 6.4 keV, Fe K $\alpha$  line, with EW up to 300 eV are, also, characteristics of the emission (de Martino et al. 2008b).

IPs are asynchronous with majority  $P_{spin}/P_{orb} \leq 0.1$  (theoretical range 0.01-0.6) (Norton et al. 2004, 2008; Scaringi et al. 2010). Polars show strong circular and linear polarization modulated at the binary period (see Beuermann 2004 for an overview). Polars, also, show asynchronicity at  $\leq 2\%$ . They have mostly short orbital periods below the period gap. Polars have a dominant soft X-ray blackbody component with  $kT \approx 10$ -30 eV (Mauche et al. 1999, Traulsen et al. 2011) due to blobby accretion and WD heating where only

about 33% has no soft component. Cyclotron cooling dominates the Bremsstrahlung cooling as the magnetic field increases and the hard X-ray tails appear at low field strengths for Polars along with soft X-ray excess increasing with magnetic field strength. Low accretion rate Polars have  $L \leq \times 10^{30}$  erg s<sup>-1</sup>. Low and high states occur due to nonuniform accretion and in any survey 50% of Polars are in a low state (Ramsay et al. 2004). MCVs show energy dependent X-ray/UV/optical pulses and harder/softer poles for a given source. MCVs show the orbital ( $\Omega$ ) and spin ( $w$ ) periods in their X-ray power spectra with appearance of sidebands (e.g.,  $2w-\Omega$ ). The power spectra of the X-ray light curves are good accretion mode diagnostics with a peak at  $w$  yielding disc fed, peaks at  $w$ ,  $w-\Omega$  yielding stream-fed accretion, together with  $w$ ,  $w-\Omega$  and  $\Omega$  appearing when disc overflow occurs as well. In addition, IPs show orbital modulations (Parker et al. 2005) which has been suggested as an effect of absorption on the binary plane.

## 3. Non-magnetic Cataclysmic Variables

In Non-magnetic CVs, the WD accretes matter from late-type MS star filling the Roche Lobe forming an accretion disk around the WD reaching all the way to the WD since the magnetic field is very low or non-existent (see Warner 1995, 2003). There are several subclasses: (1) Dwarf Novae in which matter is transferred at continuous or sporadic rates, accretion is interrupted every few weeks to months by intense accretion (outburst) of days to weeks with  $10^{39}$ - $10^{40}$  erg involved energy and the optical magnitudes change by  $\Delta m = 2$ -6; (2) Nova-like Variables with high accretion rates (3) the Classical and Recurrent Nova where explosive ignition (Thermonuclear Runaway) of accreted material on the surface of the WD occurs and material is ejected from the CV system with  $10^{43}$ - $10^{46}$  erg of energy ( $\Delta m = 9$ -10 magnitudes in the optical wavelengths).

The material in the inner disc of Non-magnetic CVs initially moving with Keplerian velocity dissipates its kinetic energy in order to accrete onto the slowly rotating

WD creating a boundary layer (BL), the transition region between the disc and the WD (see Mauche 1997 for an overview). Standard accretion disc theory predicts half of the accretion luminosity to originate from the disc in the optical and ultraviolet (UV) wavelengths and the other half to emerge from the boundary layer as X-ray and extreme UV (EUV) emission which may be summarized as  $L_{BL} \sim L_{disk} = GM_{WD}\dot{M}_{acc}/2R_{WD} = L_{acc}$  (Lynden-Bell & Pringle 1974, Godon et al. 1995). During low-mass accretion rates,  $\dot{M}_{acc} < 10^{-(9-9.5)} M_{\odot}$ , the boundary layer is optically thin (Narayan & Popham 1993, Popham 1999) emitting mostly in the hard X-rays ( $kT \sim 10^{(7.5-8.5)} K$ ). For high accretion rates,  $\dot{M}_{acc} \geq 10^{-(9-9.5)} M_{\odot}$ , the boundary layer is expected to be optically thick (Popham & Narayan 1995) emitting in the soft X-rays or EUV ( $kT \sim 10^{(5-5.6)} K$ ). Since the non-magnetic CVs are diverse, here I concentrate on dwarf nova and classical nova systems for further X-ray observations.

### 3.1. Dwarf Novae

During quiescence (low-mass accretion rates) of DN systems the boundary layer is detected in the hard X-rays. The X-ray spectra are mainly characterised with a multi-temperature isobaric cooling flow type model of plasma emission at  $T_{max} = 9-55$  keV with accretion rates of  $10^{-12}-10^{-10} M_{\odot} \text{ yr}^{-1}$ . The X-ray line spectroscopy indicates narrow emission lines (brightest OVIII  $K\alpha$ ) and near solar abundances, with a 6.4 keV line due to reflection from the surface of the WD. The detected Doppler broadening in lines during quiescence is  $< 750 \text{ km s}^{-1}$  with electron densities  $> 10^{12} \text{ cm}^{-3}$  (see Perna 2003, Baskill et al. 2005, Kuulkers et al. 2006, Rana et al. 2006, Pandel et al. 2005, Balman et al. 2011). A missing BL in the X-rays have been suggested due to low  $L_x/L_{disk}$  ratio. However, it has been pointed out that BL may emit significant fraction of its luminosity in the EUV/FUV close to the star (Sion et al. 1966, Pandel et al. 2005).

DN outbursts are brightenings of the accretion discs as a result of thermal-viscous instabilities summarized in the DIM model (Disc

Instability Model; Lasota 2001, 2004). During the outburst stage, DN X-ray spectra differ from the quiescence since the accretion rates are higher (about two orders of magnitude), the BL is expected to be optically thick emitting EUV/soft X-rays (Lasota 2001, see the X-ray review in Kuulkers et al. 2006). Soft X-ray/EUV temperatures are in a range 5-30 eV are detected from some systems (e.g., Mauche et al. 1995, Mauche & Raymond 2000). As a second emission component, DN show hard X-ray emission during the outburst stage however, at a lower flux level and X-ray temperature compared with the quiescence (e.g., WW Cet & SU UMa: Fertig et al. 2011, SS Cyg: MacGowen et al. 2004). On the other hand, some DN show increased level of X-ray emission including soft X-rays (GW Lib & U Gem: Byckling et al. 2009). The grating spectroscopy of the outburst data indicate large widths for lines with velocities in excess of  $1000 \text{ km s}^{-1}$  (Mauche 2004, Rana et al. 2006).

In the accretion process the material travels from outside inwards and any time variations of the mass transfer rate in the flow is also transported inwards. This self-similar variability of accretion rate is referred as flicker noise (Lyubarskii 1997; see also Anzolin et al. 2010 for a review for CVs). Low frequency perturbations generated at the outer disc propagate towards the WD and finally to the X-ray emitting region. Variations occur at any radii on dynamic timescales and most variability emerges from inner regions (Churazov et al. 2001). Thus, studying the broad-band noise characteristics of the power spectra from cataclysmic variables can shed light on the inner disk geometry and dynamics. Disk truncation radii for IP systems have been observationally detected this way ( $R_{in} = 1.9 \times 10^9 \text{ cm}$ , Revnivtsev et al. 2011) The missing BL as proposed from earlier results and UV/X-ray delays detected in the DN outbursts are indication of possible disk truncation in DN. Truncated accretion disks in Dwarf Novae may also help to explain quiescent brightness levels and also high  $\dot{M}$  during quiescence in some DNs. Models have been suggested where irradiation by the WD (King 1997), a coronal siphon flow (Meyer & Meyer-Hofmeister 1994, Liu et al. 1995), WDs ro-

tating near break up velocity (Ponman et al. 1995), a spherical corona (Mahasena & Osaki 1999), or a hot settling flow (Medvedev & Menou 2002) that may be responsible for the distruption of the inner disc explaining the lack of X-ray emission and formation of coronal flows.

### 3.2. Classical and Recurrent Novae

Classical novae (CNe) outbursts occur in Cataclysmic Variable (CV) systems on the surface of the WD as a result of an explosive ignition of accreted material (Thermonuclear Runaway-TNR) causing the ejection of  $10^{-7}$  to  $10^{-3} M_{\odot}$  of material at velocities up to several thousand kilometers per second (Shara 1989; Livio 1994; Starrfield 2001; Bode & Evans 2008). The classical nova systems have an initial low level accretion phase ( $\leq 10^{-11} M_{\odot}$ ) where the recurrent nova generally show higher accretion rates. Once the critical pressure at the base of the WD envelope is reached (e.g.,  $10^{19} \text{ dyn cm}^{-2}$ ) the temperatures reach  $T \sim 10^8 \text{ K}$ , a TNR occurs and the hydrogen on the surface of the WD starts burning. Next, the inverse Beta-decay reactions produce isotopes that reach the outer layers of the convective envelope dumping enough energy expanding the outer layers. In the initial expansion phase the WD envelope reaches to sizes a few  $\times 10^{12} \text{ cm}$  and a visual maximum is attained. A gradual hardening of the stellar remnant spectrum with time past visual maximum is expected consistent with H-burning at constant bolometric luminosity and decreasing photospheric radius, as the envelope mass is depleted. This residual hydrogen-rich envelope matter is consumed by H-burning and wind-driven mass loss. Some of the important parameters that govern nova evolution are the initial accretion rate, the age of the white dwarf, the mass of the white dwarf and the composition of the envelope over the white dwarf surface (Prialnik & Kovetz 1995; Starrfield et al. 1998; Yaron et al. 2005).

The emission from the remnant WD is mainly a blackbody-like stellar continuum referred as the soft X-ray component. As the stellar photospheric radius decreases in time during the constant bolometric luminosity phase, the

effective photospheric temperature increases (up to values in the range  $1-10 \times 10^5 \text{ K}$ ) and the peak of the stellar spectrum is shifted from visual to ultraviolet and to the X-ray energy band (0.1-1.0 keV), where finally the H-burning turns off (Balman et al. 1998; Balman & Krautter 2001; Orio et al. 2002; Ness et al. 2007; Nelson et al. 2008; Page et al. 2010; Rauch et al. 2010, Ness et al. 2011).

CNe is, also, detected in the hard X-rays (above 0.5 keV) as a result of shocked plasma emission *during the outburst stage* referred as the hard X-ray component. The main mechanisms responsible for this component are : (1) circumstellar interaction (Balman 2005, 2010, Bode et al. 2006, Sokoloski et al. 2006.); (2) wind-wind interaction (Mukai & Ishida 2001, Orio et al. 2005; Lynch et al. 2008, Ness et al. 2009); (3) stellar wind instabilities and X-ray emission (as in Owocki & Cohen 1999); (4) mass accretion and flickering X-ray light curves, 6.4 keV Fe lines (Hernanz & Sala 2002, 2007; Page et al. 2010). Comptonized X-ray emission from the Gamma-rays produced in radioactive decays after the TNR has been suggested as a possible hard X-ray Component (example:  $^{22}\text{Na}$ ,  $^7\text{Be}$ ,  $^{26}\text{Al}$ ; Hernanz et al. 2002).

For the soft X-ray component, originally spectral analysis were done using interstellar absorption (hydrogen column density) and blackbody emission models which yielded super-Eddington luminosities for the stellar remnant. To correct this, atmosphere models of C-O and O-Ne core WDs with LTE (Local Thermodynamic Equilibrium) were used along with interstellar absorption with the *ROSAT* and *Beppo-Sax* data (e.g, Balman, Krautter, Ögelman 1998, Balman & Krautter 2001). After the X-ray grating data were obtained, detailed emission and absorption features were detected with present observatories. Soft X-ray spectra were fitted using hydrostatic NLTE atmosphere models along with interstellar absorption by equivalent hydrogen column density (Orio et al. 2002, Nelson et al. 2008, Rauch et al. 2010, Osborne et al. 2011, Ness et al. 2011) that would account for the absorption edges/lines from a static atmosphere. However, the detailed structure in the spec-

tra was very difficult to model yielding best approximations to the observed spectra with large  $\chi^2$  values. In addition, most absorption features showed blue-shifts in the spectra (e.g. Ness et al. 2007, 2009) not modeled by the NLTE static atmosphere models. In order to compensate for this, stellar atmosphere code PHOENIX (Hauschildt & Baron 2004) was adjusted to model NLTE expanding atmosphere models, a hybrid atmosphere model that is hydrostatic at the base with an expanding envelope on top. These models have been used to fit data with yet again best approximations yielding estimated spectral parameters (e.g. Petz et al. 2005, van Rossum & Ness 2010).

#### 4. Some Recent Results and Future Prospects

In the previous sections, I reviewed a general perspective on observational X-ray properties of Cataclysmic Variables. In this section, I discuss some current research prospects relating to X-ray emission from CVs and future work.

One of the important issues of the MCVs is the modeling of the accretion shock and the column structure (i.e., density/temperature; also, stratification) and its possible variations (see Yuasa et al. 2010). Variations on the maximum temperature attained and the derived WD masses indicate that the structure in the columns may be changing. Recent work on EX Hya by Pekön & Balman 2011 reveals that the cold absorption from the bulge at the accretion impact zone and the neutral column density in the accretion column along with the covering fraction seems to be indirectly proportional. Figure 1 top panel shows the orbital phase-resolved X-ray spectra of EX Hya. In general, results indicate that as the size of the bulge gets larger, the accretion curtain size and the absorption is getting smaller. Moreover, the maximum temperature gets hotter as the absorption and the covering fraction in the accretion curtain gets smaller. In general, such changes in the intermediate polar sources suggests that shock structure in the column is not persistent and the accretion geometry in the system is also variable. This may relate to small changes on the accretion rate and the small variations in

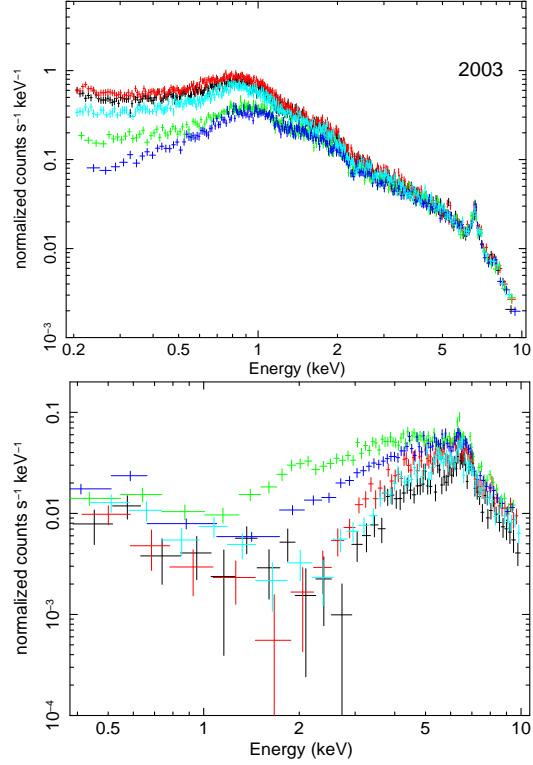


**Fig. 1.** The top figure shows the orbital-phase resolved spectra of EX Hya in 2003. The bottom figure is the orbital-phase resolved spectra of FO Aqr in 2004. Details can be found in Pekön & Balman (2011) and Balman & Pekön (2011a).

the magnetic field magnitude and geometry. It is possible that this is a general feature of the MCVs and such variations on the accretion geometry, the column temperature changes and field variations can be followed well by monitoring observations using simultaneous orbital and spin phase-resolved spectroscopy of these systems.

Another interesting class of objects within the IP class is the small group that hosts a warm absorber; V1223 Sgr, V709 Cas, and RXJ173021.5-055933 (detected from OVII K-edges). It is suggested that these absorbers exist in the pre-shock in the accretion curtain/column. However, lately the detection of the warm-absorber in the orbital phase-

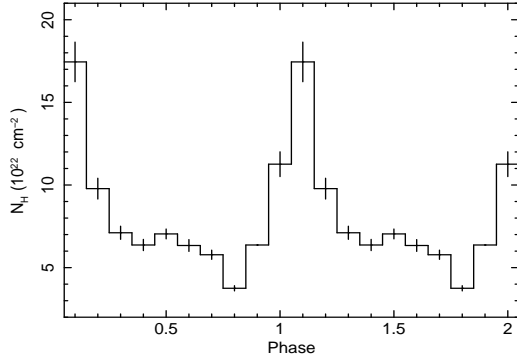


**Fig. 2.** The orbital-phase resolved neutral column density variation in the spectra FO Aqr in 2004 (Balman & Pekön 2011a).

resolved spectra of FO Aqr (see Balman & Pekön 2011a) at the bulge of the accretion impact zone reveals that just like Low-mass X-ray binary dippers CVs can have warm-absorbers on the disk. Figure 1 bottom panel shows the orbital phase-resolved X-ray spectra of FO Aqr and Figure 2 is the variation of the equivalent neutral hydrogen density over the binary phase. The minimum and maximum spectra over the orbital phase have been simultaneously fitted assuming a simple cold absorber and a *warm absorber* model given the same plasma emission components yielding  $\text{Log}(\xi) = 2.2$  ( $\xi = L/nr^2$ ) and  $N_{\text{warm}} = (6.5 \pm 1.6) \times 10^{22} \text{ cm}^{-2}$ . Present and future X-ray missions with high sensitivity can be used to reveal the structure on the disk via orbital phase-resolved spectroscopy and the pre-shock by spin phase-resolved spectroscopy which will reveal if the X-ray emission from Intermediate Polars and/or Polars are being processed and changed in the systems via ionized warm absorption in the X-rays and how this in the end effects the long and short term variation of the shock characteristics.

The X-ray emission from boundary layers have been found to be less than predicted as mentioned before. A recent work by Balman & Revnivtsev (2011, in preperation, see also Balman et al. 2011) show that for five DN systems, SS Cyg, VW Hyi, RU Peg, WW Cet and T Leo, the UV and X-ray power spectra show breaks in the variability with break fre-

quencies indicating the inner disc truncation in these systems. The truncation radii for DN are calculated in a range  $(3-10) \times 10^9 \text{ cm}$ . The authors also analyze the *RXTE* data of SS Cyg in outburst and compare it with the power spectral analysis of the quiescence data where they show that the disc moves towards the white dwarf and recedes as the outburst declines; between  $1-5 \times 10^9$  (see Figure 3) observationally for the first time. Balman & Revnivtsev (2011) also calculate the correlation between the simultaneous UV and X-ray light curves of five DNe, using *XMM-Newton* data obtained in quiescence and find time lags consistent with delays in the X-rays of 90-200 sec. The lags occur such that the UV variations lead X-ray variations which shows that as the accreting material travels onto the WD, the variations are carried from the UV into the X-ray emitting region. Therefore, the long time lags of the order of minutes can be explained by the travel time of matter from a truncated inner disk to the white dwarf surface. The same study by Balman & Revnivtsev (2011) (see also Balman et al. 2011) shows high correlation of X-ray and UV light curves around zero time lag indicating irradiation effects in these systems. In general, DN may have large scale truncated accretion disks in quiescence which can also explain the UV and X-ray delays in the outburst stage and the accretion may occur through a coronal flow in the disc (e.g., rotating accretion disk coronae). Note that extended emission and winds are detected from DN in the outburst stage which may be an indication of the coronae in these systems (e.g., Mauche 2004). It is plausible to monitor DN systems in the X-rays to measure variability in the light curves in time together with the variations of the disk truncation and formation of plausible coronae on the disk in quiescence and outburst.

The complications in modeling of the soft X-ray component of novae in outburst have been discussed in the previous section. Balman & Pekon (2011b) has used a new approach to analyze soft component of novae using a complex absorption model along with a simple blackbody model for the continuum. Main aim has been to model the absorption components detected in the high resolution spectra inde-

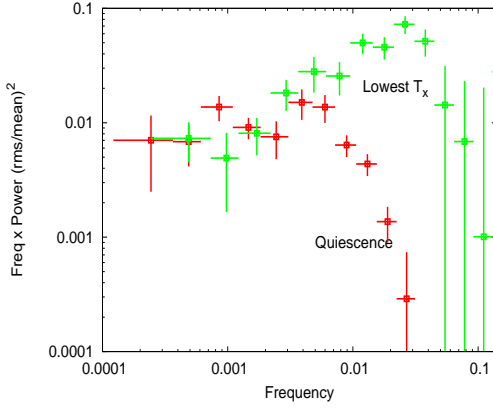


**Fig. 3.** The average Power Spectrum of the SS Cyg in quiescence and outburst when the X-ray temperatures are the lowest. The entire *RXTE* data is utilized for the analysis (Balman & Revnivtsev 2011).

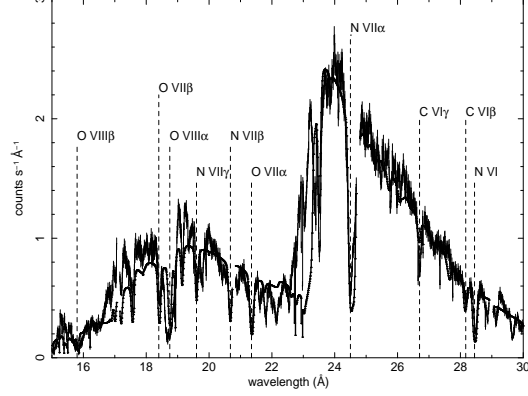


**Fig. 4.** The *XMM-Newton* RGS spectrum of V2491 Cyg fitted with the collisionally ionized hot absorber model in SPEX. Blue-shifted lines are marked on the figure (see Balman & Pekön 2011b).

pendently from the assumed continuum model. The complex absorption is of photospheric, interstellar (hydrogen column density) and of the collisionally and/or photoionized gas origin in the moving material in the line of sight from a nova wind or ejecta. The authors utilize photoionized warm absorber models and collisionally ionized hot absorber models for the analysis using the SPEX software (Kaastra et al. 1996). The results indicate blackbody temperatures that are similar to the expanding NLTE atmosphere model temperatures (for the underlying WD photospheric temperature). They model the ionized absorption features simultaneously, calculating a global velocity shift for the absorption component in the data originating from the nova wind/ejecta. Figure 4 shows the fitted *XMM-Newton* RGS data using collisionally ionized hot absorber model. A blue-shifted absorber with  $3078\text{--}3445 \text{ km s}^{-1}$  for V2491 Cyg and  $1085\text{--}1603 \text{ km s}^{-1}$  for V4743 Sgr have been calculated consistent with wind/ejecta speeds. They derive CNO abundances from the fits where V2491 Cyg has a nitrogen overabundance of  $N=14\text{--}36$  (ratio to solar abundance) and C and O are about twice their solar abundance. V4743 Sgr shows a typical signature of H-burning with under-abundant carbon  $C=0.004\text{--}0.2$ , and en-

hanced nitrogen  $N=12\text{--}53$  and oxygen  $O=24\text{--}53$  (all ratio to solar abundances). The equivalent hydrogen column density of the ionized absorbers are  $(8.0\text{--}0.3)\times 10^{22} \text{ cm}^{-2}$  for V2491 Cyg and  $(3.6\text{--}7.0)\times 10^{23} \text{ cm}^{-2}$  for V4743 Sgr. The results suggest that the RGS data of V2491 Cyg is in accordance with both a collisionally ionized absorber (e.g., shocks within winds) and photo-ionized warm absorber modeling major blue-shifted absorption features as the  $\chi^2_\nu$  are only slightly different. For V4743 Sgr, a photo-ionized warm absorber (e.g., photo-ionized wind) is a more physically consistent interpretation with relatively better  $\chi^2_\nu$  values.

This analysis can be extended to other existing data on these nova and others to see how complex absorption may have effect on X-ray spectra and how the absorbers and abundances evolve in time. In addition, one can utilize plausible different continuum atmosphere models. The systems may show different characteristics depending how deeply embedded the X-ray emitting region is inside the expanding wind/ejecta and where/how much the collisionally ionized gas dominates.

## 5. Discussion

**Simone Scaringi:** Does the high frequency break move to higher frequencies when looking at higher energies ?

**Solen Balman:** No not expected. The *RXTE*, *XMM-Newton* EPIC and OM-UV light curves show similar breaks within errors.

**Vitaly Neustroev:** Where do the orbital modulations in Intermediate Polars come from ?

**Solen Balman:** They are due to cold/warm absorption from the bulge at the accretion stream impact zone on the outer edge of the disk.

*Acknowledgements.* SB acknowledges support from TÜBİTAK, The Scientific and Technological Research Council of Turkey, through project 108T735.

## References

- Anzolin, G., et al. 2008, A&A, 489, 1243  
 Anzolin, G., Tamburini, F., de Martino, D., & Bianchini, A. 2010, A&A, 519, 69  
 Barlow, E.J., et al. 2006, MNRAS, 372, 224  
 Balman, Ş. & Pekön, Y. 2011a, in Physics of Accreting Compact Binaries, ed. D. Nogami, P. Mason, & C. Knigge (Tokyo: Universal Academy Press), in press  
 Balman, Ş. & Pekön, Y. 2011b, A&A, submitted  
 Balman, Ş., Godon, P., Sion, E. M., Ness J.,-U., Schlegel, E., Barrett, P. E., & Szkody, P. 2011, ApJ, 741, 84  
 Balman, Ş. 2010, MNRAS, 404, L26  
 Balman, Ş. 2005, ApJ, 627, 933  
 Balman, Ş., & Krautter, J. 2001, MNRAS, 326, 1441  
 Balman, Ş., Krautter, J., & Ögelman, H. 1998, ApJ, 499, 395  
 Baskill, D., Wheatley, P.J., & Osborne, J.P. 2005, MNRAS, 357, 626  
 Beuermann, K. 2004, in ASP Conf. ser. 315, IAUC 190: Magnetic Cataclysmic Variables, ed. S. Vrielmann, & M. Cropper, 187  
 Bode, M. F., & Evans, A., 2008, Classical Novae 2nd Edition, Cambridge Astrophysics Series No. 43 (Cambridge: Cambridge University Press)  
 Bode, M. F., et al. 2006, ApJ, 652, 629  
 Byckling, K., et al. 2009 MNRAS, 399, 1576  
 Brunschweiler, J., Greiner, J., Ajello, M., & Osborne, J. 2009, A&A, 496, 121  
 Churazov, E., Gilfanov, M., & Revnivtsev, M. 2001, MNRAS, 312, 759  
 Cropper, M. 1990, SSRv, 54, 195  
 de Martino, D., et al. 2008a, A&A, 481, 149  
 de Martino, D., et al. 2008b, MmSAI, 79, 246  
 Evans, P. A. & Hellier, C., 2007, ApJ, 663, 1277  
 Fertig, D., Mukai, K., Nelson, T., & Cannizzo, J.K. 2011, PASP, 123, 1054  
 Godon, P., Regev, O., & Shaviv, G. 1995, MNRAS, 275, 1093  
 Hauschildt, P.H. & Baron, E. 2004, A&A, 417, 317  
 Hellier, C. 1996, in Cataclysmic Variables and Related Objects, ed. A. Evans, J.H. Wood (Dordrecht: Kluwer), 143  
 Hernanz, M. & Sala, G. 2002, Science, 298, 393  
 Hernanz, M. & Sala, G. 2007, ApJ, 664, 467  
 Hernanz, M., Gomez-Gomar, J., & Joe, J. 2002, NewAR, 46, 559  
 Kaastra, J.S., Mewe, R., & Nieuwenhuijzen, H. 1996, in UV and X-ray Spectroscopy of Astrophysical and Laboratory Plasmas, Frontiers science series, 15, 411  
 King, A. R. 1997, MNRAS, 288, L16  
 King, A. R. & Lasota, J.P. 1979, MNRAS, 188, 653  
 Kuulkers, E., Norton, A., Schwöpe, A., & Warner, B. 2006, in Compact stellar X-ray sources, ed. W. Lewin & M. van der Klis, Cambridge Astrophysics Series No. 39 (Cambridge, UK: Cambridge University Press), 421  
 Lamb, D.Q. & Masters, A.R. 1979, ApJ, 234, L117  
 Landi, R., et al. 2009, MNRAS, 392, 630  
 Lasota, J. P. 2001, NewAR, 45, 449  
 Lasota, J. P. 2004, RMxAC, 20, 124  
 Livio, M. 1994, in Interacting Binaries, Saas-Fee Advanced Course 22, ed. H. Nussbaumer, & A. Orr (Berlin: Springer), 135  
 Liu, F. K., Meyer, F., & Meyer-Hofmeister, E. 1995, A&A, 300, 823  
 Luna, G. J. M., et al. 2010, ApJ, 711, 1333  
 Lynch, D. K., et al. 2008, AJ, 136, 1815  
 Lynden-Bell, D. & Pringle, J. E. 1974, MNRAS, 168, 603



- Lyubarskii, Y. E. 1997, *MNRAS*, 292, 679
- Mahasena, P. & Osaki Y. 1999, *PASJ*, 51, 45
- Mauche, C. W. 2004, *ApJ*, 610, 422
- Mauche, C. W., & Raymond, J. C. 2000, *ApJ*, 541, 924
- Mauche, C. W. 1999, in *ASP Conf. Ser.* 157, *Annapolis Workshop on Magnetic Cataclysmic Variables*, ed. C. Helier & K. Mukai, 157
- Mauche, C. W. 1997, in *X-ray imaging and spectroscopy of hot plasmas*, ed. F. Makino & K. Mitsuda, *Proceedings of an International Symposium on X-ray Astronomy ASCA Third Anniversary*, 529
- Mauche, C. W., Raymond, J. C., Mattei, J. A. 1995, *ApJ*, 446, 842
- McGowan, K.E., Priedhorsky, W.C., & Trudolyubov, S. P. 2004, *ApJ*, 601, 1100
- Medvedev, M., & Menou, K. 2002, *ApJ*, 565, L39
- Meyer, F., & Meyer-Hofmeister, E. 1994, 288, 175
- Mukai, K., Kinkhabwala, A., Peterson, J. R., Kahn, S. M., & Paerels F. 2003, *ApJ*, 586, 77
- Mukai, K., & Ishida, M. 2001, *ApJ*, 551, 1024
- Narayan, R., & Popham, R. 1993, *Nature*, 362, 820
- Nelson, T., et al. 2008, *ApJ*, 673, 1067
- Ness, J.-U., et al. 2009, *AJ*, 137, 3414
- Ness, J.-U., et al. 2007, *ApJ*, 665, 1334
- Ness, J.-U. 2010, *AN*, 331, 179
- Ness, J.-U., et al. 2011, *ApJ*, 733, 70
- Norton, A.J., Wynn, G.A., & Somerscales, R.V. 2004, *ApJ*, 614, 349
- Norton, A.J., Butters, O. W., Parker, T. L., & Wynn, G. A. 2008, *ApJ*, 672, 524
- Orio, M., et al. 2002, *MNRAS*, 333, L11
- Orio, M., Tepedelenlioglu, E., Starrfield, S., Woodward, C. E., & Della Valle, M. 2005, *ApJ*, 620, 938
- Osborne, J.P., et al. 2011, *ApJ*, 727, 124
- Owocki, S.P. & Cohen, D.H. 1999, *ApJ*, 520, 833
- Paterson, J. 1994, *PASP* 106, 209
- Page, K.L., et al. 2010, *MNRAS*, 401, 121
- Pandel, D., Córdova, F.A., Mason, K.O., & Priedhorsky, W.C. 2005, *ApJ*, 626, 396
- Parker, T. L., Norton, A. J., & Mukai, K. 2005, *A&A*, 439, 213
- Patterson, J. 1994, *PASP*, 106, 209
- Pekön, Y., & Balman, S. 2011, *MNRAS*, 411, 1177
- Petz, A., Hauschildt, P.H., Ness, J.-U., & Starrfield S. 2005, *A&A*, 431, 321
- Perna, R., McDowell, J., Menou, K., Raymond, J., & Medvedev, M. 2003, *ApJ*, 598, 545
- Prialnik, D., Kovetz, A. 1995, *ApJ*, 445, 789
- Pretorius, M.L., Knigge, C. 2011, *MNRAS*, in press
- Ponman, T. J., et al. 1995, *MNRAS*, 276, 495
- Popham, R., & Narayan, R. 1995, *ApJ*, 442, 337
- Popham, R. 1999, *MNRAS*, 308, 979
- Ramsay, G., Cropper, M., Wu, K., Mason, K. O., Córdova, F., & Priedhorsky, W. 2004, *MNRAS*, 350, 1373
- Rana, V. R., Singh, K. P., Schlegel, E. M., & Barrett, P. E., *AdSpR*, 38, 2847
- Revnivtsev, M., et al., 2010, *A&A*, 513, 63
- Revnivtsev, M., Potter, S., Kniazev, A., Burenin, R., Buckley, D.A.H., & Churazov, E. 2011, *MNRAS*, 411, 1317
- Rauch, T., et al. 2010, *ApJ*, 717, 363
- van Rossum, D.R., Ness, J.-U. 2010, *AN*, 331, 75
- Sazonov, S., et al. 2006, *A&A*, 450, 117
- Shara, M. M. 1989, *PASP*, 101, 5
- Sokoloski, J. L., Luna, G. J. M., Mukai, K., & Kenyon, S. J. 2006, *Nature*, 442, 276
- Starrfield, S. 2001, in *ASP Conf. Ser.* 231, *Tetons 4: Galactic Structure, Stars, and the Interstellar Medium*, ed. C.E. Woodward, M.D. Bica, & J.M. Shull (San Francisco: ASP), 466
- Starrfield, S., Truran, J. W., Wiescher, M. C., Sparks, W. M. 1998, *MNRAS*, 296, 502
- Scaringi, S., et al. 2010, *MNRAS*, 401, 2207
- Sion, E. M., Cheng, F., Huang, M., Hubeny, I., & Szkody, P. 1996, *ApJ*, 471, L41
- Staude, A., et al. 2008, *A&A*, 486, 899
- Traulsen, I., et al. 2011, *A&A*, 529, 116
- Warner B. 1995, *Cataclysmic Variable Stars* (Cambridge: Cambridge Univ. Press)
- Warner B. 2003, *Cataclysmic Variable Stars* (Cambridge: Cambridge Univ. Press)
- Yaron, O., Prialnik, D., Shara, M. M., & Kovetz, A. 2005, *ApJ*, 623, 398
- Yuasa, T., et al. 2010, *A&A*, 520, 25